

# Generation of high power pulsed terahertz radiation using a plasmonic photoconductive emitter array with logarithmic spiral antennas

Christopher W. Berry,<sup>1</sup> Mohammad R. Hashemi,<sup>1,2</sup> and Mona Jarrahi<sup>1,2</sup>

<sup>1</sup>Department of Electrical Engineering and Computer Science, University of Michigan, Ann Arbor, Michigan 48109, USA

<sup>2</sup>Department of Electrical Engineering, University of California, Los Angeles, California 90095, USA

(Received 1 December 2013; accepted 12 February 2014; published online 27 February 2014)

An array of  $3 \times 3$  plasmonic photoconductive terahertz emitters with logarithmic spiral antennas is fabricated on a low temperature (LT) grown GaAs substrate and characterized in response to a 200 fs optical pump from a Ti:sapphire mode-locked laser at 800 nm wavelength. A microlens array is used to split and focus the optical pump beam onto the active area of each plasmonic photoconductive emitter element. Pulsed terahertz radiation with record high power levels up to 1.9 mW in the 0.1–2 THz frequency range is measured at an optical pump power of 320 mW. The record high power pulsed terahertz radiation is enabled by the use of plasmonic contact electrodes, enhancing the photoconductor quantum efficiencies, and by increasing the overall device active area, mitigating the carrier screening effect and thermal breakdown at high optical pump power levels. © 2014 AIP Publishing LLC. [<http://dx.doi.org/10.1063/1.4866807>]

Photoconductive antennas are one of the most promising and commonly used means of terahertz generation,<sup>1–9</sup> mainly due to availability of high performance and compact optical sources with pulsed and continuous-wave operation required for broadband and narrowband terahertz generation. Another valuable characteristic of photoconductive terahertz emitters is that their quantum efficiency is not limited by the Manley Rowe limit<sup>10</sup> and, therefore, can offer much higher quantum efficiencies compared to terahertz emitters based on nonlinear optical phenomena. In spite of this great potential, the inherent tradeoff between high quantum efficiency and ultrafast operation in conventional photoconductors severely limits the optical to terahertz conversion efficiency of conventional photoconductive terahertz emitters.

Recently, it has been demonstrated that incorporation of plasmonic contact electrodes can mitigate the inherent tradeoff between high quantum efficiency and ultrafast operation in conventional photoconductors.<sup>11–17</sup> This is because of the unique capability of plasmonic electrodes to enhance photocarrier concentration near photoconductor contact electrodes, allowing a larger number of photocarriers to reach the photoconductor contact electrodes within a terahertz oscillation cycle to efficiently contribute to terahertz wave generation. This unique capability has enabled significant enhancements in the optical to terahertz conversion of photoconductive emitters.<sup>18–20</sup>

The concept of optical-to-terahertz conversion efficiency enhancement through use of plasmonic contact electrodes is universal and can be utilized to enhance the optical-to-terahertz conversion efficiency of photoconductive emitters with any choice of the terahertz radiating antenna, bias feed, and photo-absorbing substrate. Here, we demonstrate a plasmonic photoconductive emitter array with logarithmic spiral antennas that generates record high pulsed terahertz radiation power by extending the antenna bandwidth and by mitigating the carrier screening effect<sup>21</sup> and thermal breakdown<sup>22</sup> at high optical pump powers. Under a 320 mW optical pump power, the emitter generates

1.9 mW of pulsed terahertz radiation in the 0.1–2 THz range.

Figure 1(a) shows the microscope image of a plasmonic photoconductive emitter element of the implemented array on a low-temperature grown (LT) GaAs substrate with a carrier lifetime of  $\sim 400$  fs. When operating in pulsed mode, since the terahertz radiating antenna is being driven by a broadband pulse of electrical current, the ideal antenna should be chosen to offer a broadband radiation resistance while maintaining a reactance value near  $0 \Omega$ .<sup>21,22</sup> For this purpose, a logarithmic spiral antenna is designed and integrated with plasmonic contact electrodes for efficient terahertz generation over a broad frequency range.<sup>23,24</sup> The logarithmic spiral antenna is designed to offer a broadband radiation resistance of 70–100  $\Omega$  and a relatively low reactance level over the 0.1–2 THz range, as shown in Fig. 2(a).

Figure 1(b) shows the scanning electron microscope (SEM) image of the plasmonic contact electrodes. Each contact electrode of the plasmonic photoconductive emitter is a plasmonic grating covering a  $30 \times 30 \mu\text{m}^2$  area. The plasmonic contact electrode gratings (pitch = 225 nm, metal width = 125 nm, metal height = 50 nm) are designed to maximize device quantum efficiency at optical pump wavelength of 800 nm.<sup>18,19</sup> The end-to-end spacing between the anode and cathode contact electrodes is set to  $30 \mu\text{m}$  to maintain the highest photocarrier drift velocity across the entire  $30 \times 30 \mu\text{m}^2$  plasmonic contact electrode area.<sup>18,20</sup>

The fabrication process started with patterning plasmonic contact electrode gratings using electron-beam lithography followed by deposition of Ti/Au (5/45 nm) and liftoff. A 150 nm SiO<sub>2</sub> passivation layer was then deposited using plasma-enhanced chemical vapor deposition. Next, contact vias were patterned using optical lithography and opened using dry plasma etching. Finally, the logarithmic spiral antennas and bias lines were patterned using optical lithography, followed by deposition of Ti/Au (10/400 nm) and liftoff.

The plasmonic photoconductive emitter with logarithmic spiral antenna is characterized in response to a 200 fs

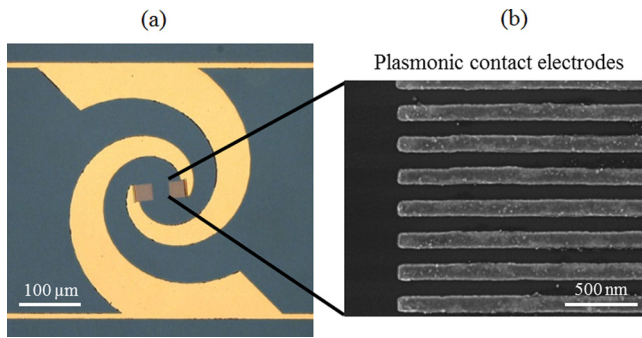


FIG. 1. Fabricated logarithmic spiral antenna integrated with plasmonic contact electrodes on a LT-GaAs substrate. (a) Microscope image of the spiral antenna. (b) SEM image of the plasmonic contact electrodes.

optical pump from a Ti:sapphire mode-locked laser at 800 nm wavelength. The optical pump is focused asymmetrically on the  $30 \times 30 \mu\text{m}^2$  anode plasmonic contact electrode to maximize device quantum efficiency by concentrating the majority of photo-generated electrons in close proximity to the anode electrode and by maintaining a high impedance loading to the logarithmic spiral antenna.<sup>18,25</sup> The relatively large device active area of  $30 \times 30 \mu\text{m}^2$  allows the optical pump power density to be maintained at relatively low levels under high optical pump power levels and, thus, enables

high power terahertz generation by mitigating the carrier screening effect and thermal breakdown at high optical pump power levels.

The radiated power from the plasmonic photoconductive emitter with logarithmic spiral antenna is measured as a function of the optical pump power and bias voltage (Fig. 2(b)) using a pyroelectric detector. At an optical pump power of 20 mW, a single emitter element radiates  $100 \mu\text{W}$  of terahertz power at a bias voltage of 40 V,  $\sim 4$  times higher than the radiated power offered by previously demonstrated plasmonic photoconductive emitters with bowtie antenna.<sup>18</sup> This significant radiation power enhancement is mainly due to use of the logarithmic spiral antenna, which offers a very broadband radiation resistance while maintaining a relatively low reactance value (Fig. 2(a)).

The radiated electric field from the plasmonic photoconductive emitter is characterized in a time-domain terahertz spectroscopy setup with electro-optic detection in a 1 mm thick ZnTe crystal.<sup>19</sup> The measured time-domain and frequency-domain radiation are shown in Figs. 3(a) and 3(b), respectively, indicating terahertz radiation over a bandwidth of more than 2 THz. It should be noted that the detection bandwidth of the terahertz spectroscopy setup is limited by the thickness of the ZnTe crystal<sup>26</sup> and; therefore, the actual radiation bandwidth is expected to be broader than that shown in Fig. 3(b).

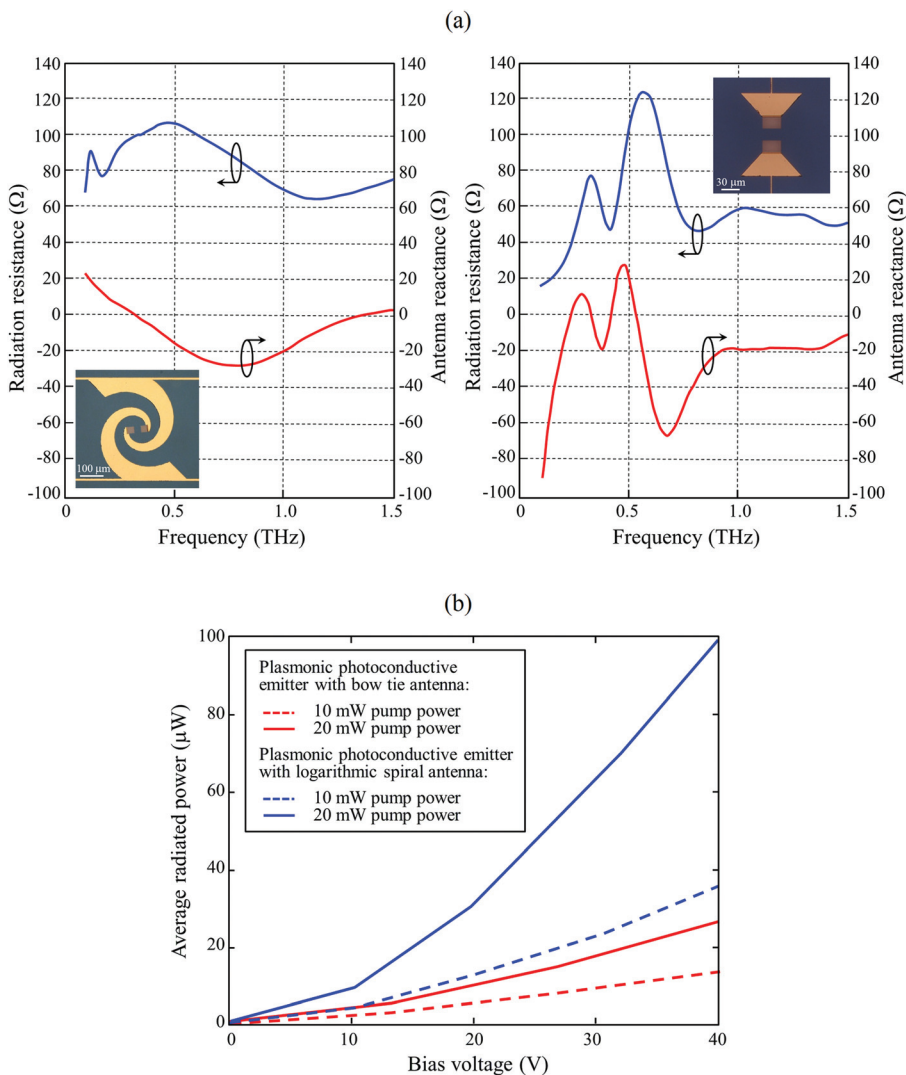


FIG. 2. (a) Radiation resistance (blue curves) and antenna reactance (red curves) for the designed logarithmic spiral antenna (left) in comparison with a bowtie antenna (right) calculated using a finite-element-based full-wave electromagnetic solver (ANSYS HFSS), (b) Radiated power from the logarithmic spiral photoconductive emitter with plasmonic contact electrodes in comparison with a comparable bowtie photoconductive emitter with plasmonic contact electrodes.

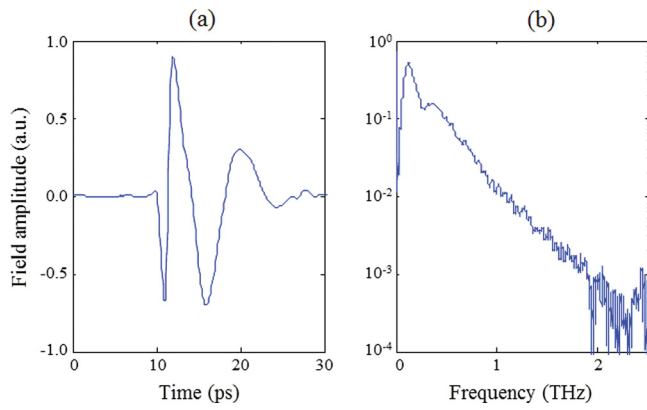


FIG. 3. Measured radiated electric field in the (a) time-domain and (b) frequency-domain.

We implemented a two dimensional array of the plasmonic photoconductive terahertz emitters with logarithmic spiral antennas, which further increases the power of the generated terahertz pulses by not only extending the antenna bandwidth but also by mitigating the carrier screening effect and thermal breakdown at high optical pump powers.<sup>27–29</sup> Figure 4(a) shows the schematic diagram and microscope image of the implemented terahertz emitter, which consists of a  $3 \times 3$  array of plasmonic photoconductive emitters with logarithmic spiral antennas. A plano-convex parabolic microlens array from Edmund Optics with  $500 \mu\text{m}$  pitch and 13.8 mm focal length is used to simultaneously split and focus portions of the optical pump beam onto the active area of each plasmonic photoconductive emitter in the  $3 \times 3$  array. For efficient optical focusing, the pitch of the antenna array is designed to match that of the microlens array at  $500 \mu\text{m}$ . The logarithmic spiral antennas, the bias lines, and plasmonic contact electrodes are identical in the array, offering a broadband radiation resistance of  $70\text{--}100 \Omega$  over the  $0.1\text{--}2$  THz range and efficient optical pump transmission through the plasmonic electrodes into the LT-GaAs substrate.

To pump the  $3 \times 3$  plasmonic photoconductive emitter array, the microlens array is mounted on a motorized rotation mount. The fabricated plasmonic photoconductive emitter is mounted on a motorized XYZ translation stage for precise alignment, and the optical alignment of the microlens and terahertz emitter array are optimized iteratively using computer control. The radiated power of the plasmonic photoconductive emitter array is shown in Fig. 4(b). Up to 1.9 mW of terahertz power is measured at an optical pump power of 320 mW and bias voltage of 100 V. Since the incident optical pump beam on the microlens array has a Gaussian spatial profile, the optical power incident upon the center device in the array is significantly higher than that of the surrounding devices. By only applying the bias voltage to the center  $1 \times 3$  plasmonic photoconductive emitter array, we observe that approximately 50% of the total emitted power from the  $3 \times 3$  plasmonic photoconductive emitter array is generated by the middle row of the array. The radiation power and optical-to-terahertz conversion efficiency of the presented plasmonic photoconductive emitter array can be enhanced even further by increasing the overall array size and/or distributing the optical pump power more evenly across the photoconductive emitter elements.

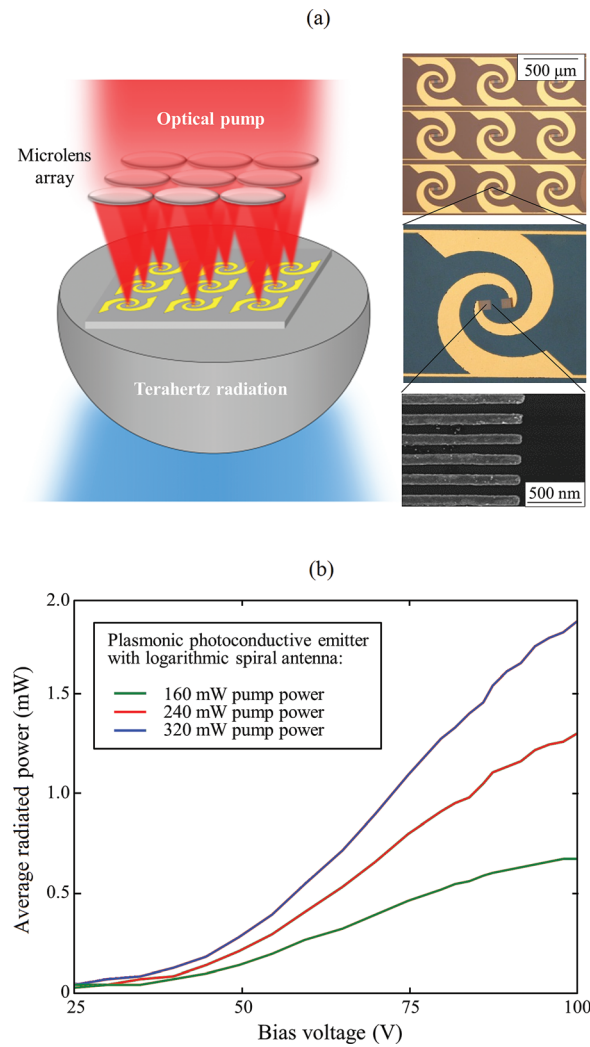


FIG. 4. (a) Plasmonic photoconductive terahertz emitter array. A microlens splits and focuses the optical pump beam onto the active area of each plasmonic photoconductive emitter element. The emitter array is mounted on a hyper-hemispherical silicon lens through which the terahertz radiation emits. (b) Radiated power from a  $3 \times 3$  plasmonic photoconductive emitter array as a function of optical pump power and bias voltage.

In summary, we experimentally demonstrate generation of record high pulsed terahertz radiation power from a  $3 \times 3$  array of plasmonic photoconductive terahertz emitters based on logarithmic spiral antennas. At an optical pump power of 320 mW, we generate 1.9 mW of pulsed terahertz radiation in the  $0.1\text{--}2$  THz frequency range. Similar to previously demonstrated plasmonic photoconductive terahertz emitters, the presented photoconductive emitter takes advantage of the enhanced device quantum efficiency enabled by the enhanced photocarrier concentration near the plasmonic contact electrodes. Compared to the previously demonstrated plasmonic photoconductive terahertz emitters, the presented photoconductive emitter offers significantly higher power terahertz pulses by extending the antenna bandwidth and by mitigating the carrier screening effect and thermal breakdown at high optical pump powers. The radiation power of the presented terahertz emitter can be further enhanced by incorporating high aspect ratio plasmonic contact electrodes<sup>30,31</sup> and by increasing the number of the plasmonic photoconductive emitter array elements, which further enhance the device quantum efficiency and

mitigate the carrier screening effect and thermal breakdown at high optical pump power levels.

The authors gratefully acknowledge the financial support from Michigan Space Grant Consortium, DARPA Young Faculty Award (# N66001-10-1-4027), NSF CAREER Award (# N00014-11-1-0096), ONR Young Investigator Award (# N00014-12-1-0947), and ARO Young Investigator Award (# W911NF-12-1-0253).

- <sup>1</sup>D. H. Auston, K. P. Cheung, and P. R. Smith, *Appl. Phys. Lett.* **45**, 284 (1984).
- <sup>2</sup>S. Preu, G. H. Döhler, S. Malzer, L. J. Wang, and A. C. Gossard, *J. Appl. Phys.* **109**, 061301 (2011).
- <sup>3</sup>J. Bjarnason, J. Chan, A. W. M. Lee, E. R. Brown, D. C. Driscoll, M. Hanson, A. C. Gossard, and R. E. Muller, *Appl. Phys. Lett.* **85**, 3983 (2004).
- <sup>4</sup>E. Peytavit, S. Lepilliet, F. Hindle, C. Coinon, T. Akalin, G. Ducournau, G. Mouret, and J.-F. Lampin, *Appl. Phys. Lett.* **99**, 223508 (2011).
- <sup>5</sup>H. Roehle, R. J. B. Dietz, H. J. Hensel, J. Böttcher, H. Künzel, D. Stanze, M. Schell, and B. Sartorius, *Opt. Express* **18**, 2296 (2010).
- <sup>6</sup>Z. D. Taylor, E. R. Brown, J. E. Bjarnason, M. P. Hanson, and A. C. Gossard, *Optics Letters* **31**, 1729 (2006).
- <sup>7</sup>M. Jarrahi, *Photon. Technol. Lett.* **21**, 830 (2009).
- <sup>8</sup>M. Beck, H. Schäfer, G. Klatt, J. Demsar, S. Winnerl, M. Helm, and T. Dekorsy, *Opt. Express* **18**, 9251 (2010).
- <sup>9</sup>S. Preu, M. Mittendorff, H. Lu, H. B. Weber, S. Winnerl, and A. C. Gossard, *Appl. Phys. Lett.* **101**, 101105 (2012).
- <sup>10</sup>P. N. Butcher and D. Cotter, *The Elements of Nonlinear Optics* (Cambridge University Press, Cambridge, U. K., 1990).
- <sup>11</sup>S.-G. Park, K. H. Jin, M. Yi, J. C. Ye, J. Ahn, and K.-H. Jeong, *ACS Nano* **6**, 2026 (2012).
- <sup>12</sup>S. Liu, X. Shou, and A. Nahata, *IEEE Trans. Terahertz Sci. Technol.* **1**, 412 (2011).
- <sup>13</sup>S.-G. Park, Y. Choi, Y.-J. Oh, and K.-H. Jeong, *Opt. Express* **20**, 25530 (2012).
- <sup>14</sup>N. Wang, M. R. Hashemi, and M. Jarrahi, *Opt. Express* **21**, 17221 (2013).
- <sup>15</sup>B. Heshmat, H. Pahlevaninezhad, Y. Pang, M. Masnadi-Shirazi, R. B. Lewis, T. Tiedje, R. Gordon, and T. E. Darcie, *Nano Lett.* **12**, 6255 (2012).
- <sup>16</sup>C. W. Berry and M. Jarrahi, Proc. Conf. Lasers and Electro-Optics, paper CFI2, San Jose, CA, May 16–21 (2010).
- <sup>17</sup>C. W. Berry and M. Jarrahi, Proc. Int. Conf. Infrared, Millimeter, and Terahertz Waves, Houston, TX, October 2–7 (2011).
- <sup>18</sup>C. W. Berry, N. Wang, M. R. Hashemi, M. Unlu, and M. Jarrahi, *Nat. Commun.* **4**, 1622 (2013).
- <sup>19</sup>C. Berry, M. R. Hashemi, M. Unlu, and M. Jarrahi, *J. Vis. Exp.* (77), e50517 (2013).
- <sup>20</sup>C. W. Berry and M. Jarrahi, *New J. Phys.* **14**, 105029 (2012).
- <sup>21</sup>G. C. Loata, M. D. Thomson, T. Löffler, and H. G. Roskos, *Appl. Phys. Lett.* **91**, 232506 (2007).
- <sup>22</sup>A. W. Jackson, J. P. Ibbetson, A. C. Gossard, and U. K. Mishra, *Appl. Phys. Lett.* **74**, 2325–2327 (1999).
- <sup>23</sup>Y. Huo, G. W. Taylor, and R. Bansal, *J. Infrared Millimeter Waves* **23**, 819 (2002).
- <sup>24</sup>E. R. Brown, A. W. M. Lee, B. S. Navi, and J. E. Bjarnason, *Microwave Opt. Technol. Lett.* **48**, 524 (2006).
- <sup>25</sup>C. W. Berry and M. Jarrahi, *J. Infrared, Millimeter Terahertz Waves* **33**, 1182 (2012).
- <sup>26</sup>J. Shan, A. Nahata, and T. F. Heinz, *J. Nonlinear Opt. Phys. Mater.* **11**, 31 (2002).
- <sup>27</sup>G. Matthäus, S. Nolte, R. Hohmuth, M. Voitsch, W. Richter, B. Pradarutti, S. Riehemann, G. Notni, and A. Tünnermann, *Appl. Phys. Lett.* **93**, 091110 (2008).
- <sup>28</sup>B. Pradarutti, R. Muller, W. Freese, G. Matthäus, S. Riehemann, G. Notni, S. Nolte, and A. Tünnermann, *Opt. Express* **16**, 18443 (2008).
- <sup>29</sup>S. T. Bauerschmidt, G. H. Döhler, H. Lu, A. C. Gossard, S. Malzer, and S. Preu, *Opt. Lett.* **38**, 3673 (2013).
- <sup>30</sup>S.-H. Yang and M. Jarrahi, *Opt. Lett.* **38**, 3677 (2013).
- <sup>31</sup>B.-Y. Hsieh and M. Jarrahi, *J. Appl. Phys.* **109**, 084326 (2011).

Applied Physics Letters is copyrighted by the American Institute of Physics (AIP).  
Redistribution of journal material is subject to the AIP online journal license and/or AIP  
copyright. For more information, see <http://ojps.aip.org/aplo/aplcr.jsp>